

Phase behavior of correlated random copolymers

Elena Patyukova* and Mark R. Wilson

Chemistry Department, Durham University, Durham, DH1 3LE, UK

Erte Xi

Proctor&Gamble, Mason Business Center,

8700 Mason Montgomery Road, Mason, Ohio, US

Abstract

In this work, Flory-Huggins phase diagrams for correlated random copolymers with realistic chain lengths are calculated. This is achieved in two steps. At first we derive a distribution function of copolymer chains with respect to composition and blockiness. Then we used the method of moments, which was developed by Sollich and Cates [Sollich, P.; Cates, M. E.; Phys. Rev. Lett. 1998, 80, 1365–1368] for polydisperse systems, to reduce the number of degrees of freedom of the computational problem and calculate phase diagrams. We explored how location of transition points and composition of coexisting phases depend on copolymer composition, blockiness and degree of polymerisation. The proposed approach allows to take into account fractionation, which was shown to have effect on the appearance of phase diagrams of statistical copolymers.

Keywords: random copolymer, Markov copolymer, phase behavior, polydispersity

* Correspondence email address: patyukova@gmail.com

I. INTRODUCTION

Random copolymers, or statistical copolymers, are polymers composed of at least two monomer units connected to each other in a more or less random manner. Random copolymers are ubiquitous in industrial applications. For example, polyvinyl alcohol (PVA) is used for creation of water-soluble pouches and capsules. PVA is obtained by post polymerisation modification from polyvinyl acetate (PVAc), in which the acetate groups can be either, fully or partially transformed into alcohol groups[1, 2]. Pure PVA films with a high degree of hydrolysis are brittle and difficult to dissolve because of considerable degree of crystallinity[3]. Lowering degree of hydrolysis or adding plasticizers leads to more flexible and soluble PVA films. To understand conditions of stability of these films with respect to segregation and their physical properties it is important to take into account a copolymer nature of PVA[4, 5].

Other examples of statistical copolymers include carboxymethyl cellulose (CMC)[6], acrylonitrile butadiene styrene (ABS), styrene-butadiene rubber (SBR), membrane electrolyte polymers like Nafion[7], polyurethanes[8] and many other commercial materials. The ability to predict polymer material properties based on their chemistry, chain structure and preparation method is crucial for product design and other industrial applications.

Molecular structure of statistical AB copolymers is most commonly characterized by the composition (i.e. the fraction of A units). Composition totally describes an ensemble of sequences in the case where there are no correlations between the type of segments at different positions along the chain. In this case, copolymers are called *random*. If there is a correlation between appearance of different types of segments at different positions along a chain then statistical copolymers are called *correlated*. Correlated copolymers can be described macroscopically in terms of concentrations of duplets (AA, BB, AB, BA), triplets (AAA, AAB, etc.), etc. The more concentrations of n-tuplets is needed to fully describe the system, the less randomness there is in a copolymer sequence. Here we consider the situation when only the composition and the concentration of duplets are enough to characterise the copolymer. If the concentration of AB-duplets in a copolymer sequence is reduced, compared to a truly random copolymer, then such correlated copolymer is referred to as a *blocky* copolymer, meaning that segments of one type tend to be arranged in *blocks*. In the opposite, case when a copolymer sequence is enriched in AB-duplets, the copolymer is called *alternating*.

In case of PVA, the degree of blockiness of PVA depends on the synthetic route [1, 2]. Saponification of PVA leads to blocky copolymers, while acetylation of previously hydrolysed PVA produces more random sequences. Appearance of correlations during saponification is due to a larger reaction constant for hydrolysing a VAc segments whose neighbours have already been hydrolysed. [2, 9].

Blocky or alternating copolymers are also common results of sequential polymerisation [10]. In this case blockiness arises when $k_{AA} \gg k_{AB}$ and $k_{BB} \gg k_{BA}$, where k_{IJ} is the reaction rate coefficient describing addition of I-segment to the growing chain with segment J at the end.

Both models belong to the class of the first-order Markov models and with the assumption that copolymerisation is stationary (concentrations of monomers are kept fixed), both produce the same types of sequences.

The equilibrium phase behavior of statistical copolymers is rich and is not yet fully understood. Early works on phase behaviour of random copolymers[11–13] concentrated on considering Flory-Huggins mixtures or copolymers with different compositions (fractions of A-segments in AB-copolymer). As the Flory-Huggins parameter, χ describing interactions between dissimilar segments, increased, an initially homogeneous mixture of copolymer chains separated into two phases with different compositions. Location of a spinodal point, with respect to separation into two phases was predicted by Scott: [11] $\chi_s = \frac{1}{\rho_2 - \rho_1^2}$ where ρ_2 and ρ_1 were correspondingly the second and the first moment of the distribution with respect to composition. Nesarikar *et al.*[13] went further and calculated phase diagrams with cloud points and compositions of coexisting phases for short Bernoulli copolymers. They showed that as the Flory-Huggins parameter, χ , increased, separation into two, three, four, etc. phases occurred. Importantly, it was also shown that distributions with respect to composition in coexisting phases in general had different shapes, in other words fractionation took place. However, these predictions and calculations were made only for polymers with small number of segments, $N \approx 10 - 30$, and no correlations along the sequence.

Another approach to predict the phase behavior of random copolymers was proposed by Shakhnovich and Gutin[14] and later developed by other authors [15–21]. It was based on Landau expansion of the free energy of a copolymer melt in terms of the order parameter representing a deviation of a local composition from a global composition. Coefficients of ex-

pansion were calculated within a mean-field approximation and expressed through single-chain correlation functions averaged over all sequences. This approach was applied to correlated random copolymers by Fredrickson *et al.*[15]. It was shown that an initially homogeneous melt of blocky copolymers separated first into two macrophases upon increase in Flory-Huggins parameter. This transition was closely followed by remixing and forming one microphase separated phase with no long-range order. The period of the microphase had a strong dependence on the temperature and decreased as $L \sim (T_s - T)^{-1/2}$ as temperature decreased. For alternating copolymers, a critical value of sequence correlation λ_C was found, such that for $\lambda < \lambda_C$ a direct transition from homogeneous state into microphase separated state was predicted, without macrophase separation.[15]

Nesarikar *et al.* [13] pointed out that one features of Shakhnovich-Fredrickson approach was that it did not take fractionation into account. It implicitly assumed that the distribution with respect to compositions had the same shape and only the mean value of composition had been changed. This assumption was too strong for non-symmetric comopolymers. Their another prediction was that for sufficiently short copolymers, $N \lesssim 60$, transition to microphase should be preceded by coexistence of three macrophases.

Recently this discussion was continued by von der Heydt *et al.*[22] who considered a mixture of triblock copolymers, AAA, BBB, ABB, AAB, BAB, ABA, with overall composition $f = 0.5$ and varied volume fractions of different sequences to imitate Markovian sequence correlations. They showed that as the Flory-Huggins parameter, χ , increased coexistence of two A- and B-rich macrophases was followed by coexistence of three phases one of which was lamellar microphase. Microphase emerged as a shadow phase and was enriched in alternating sequences. So, both microphase separation and threephase coexistence took place simultaneously.

The latest results show that it is important to take fractionation into account to make a correct prediction of phase behavior[23]. In this work, we aim at taking into account fractionation in the framework of Flory-Huggins theory of blocky copolymers with realistic chain lengths. Therefore, we consider only the possibility of macrophase separation despite knowing about the existence and importance of microphase separation in statistical copolymers. This is done to get a solid reference point for a more refined picture including microphase separation, which may be developed in the future.

In this work we use the method of moments proposed by Sollich *et al.*[24] for polydisperse systems. This method can effectively reduce the number of degrees of freedom of polydisperse system, otherwise the system consist of, an order of magnitude, 2^N different components and direct solution of the phase equilibrium equations is not possible. To use the method of moments we derive the probability distribution function of copolymer chains with respect to composition and blockiness. Then we obtain Flory-Huggins phase diagrams of blocky copolymers and study the dependence of phase diagrams on the composition of copolymer, chain length and degree of correlations along the sequence. At the end we make comparison of our results with the work of Nesarikar *et al.*[13] and Fredrickson *et al.*[15].

The paper is organised as follows. First, we derive a distribution function for correlated copolymers. Then we feed this distribution into the moments method and obtain phase diagrams, volumes of coexisting phases and their density distributions.

II. DERIVATION OF A DISTRIBUTION FUNCTION FOR MARKOV COPOLYMERS

In order to derive a distribution function for Markov polymers of the first order let's first look at AB random binomial copolymers with chain length N , the number of A-monomers equal to N_A and their average fraction $f = \langle N_A/N \rangle$ in the population of copolymer chains. The distribution function can be written as:

$$\rho(N_A) = \frac{N!}{N_A!(N - N_A)!} f^{N_A} (1 - f)^{N - N_A} \quad (1)$$

. Or if we use Stirling's formula $N! \approx \sqrt{2\pi N} \left(\frac{N}{e}\right)^N$ and introduce $\sigma = \frac{N_A}{N}$,

$$\begin{aligned} \rho(\sigma) &= \frac{1}{\sqrt{2\pi N \sigma (1 - \sigma)}} \left(\frac{f}{\sigma}\right)^{N\sigma} \left(\frac{1 - f}{1 - \sigma}\right)^{N - N\sigma} \sim \\ &\sim \frac{1}{\sqrt{2\pi N f (1 - f)}} \left(\frac{f}{\sigma}\right)^{N\sigma} \left(\frac{1 - f}{1 - \sigma}\right)^{N - N\sigma} \end{aligned} \quad (2)$$

Let us consider now an infinite random AB sequence characterised by the fraction of A-segments, f . Then we can write down an information entropy per monomer of such sequence:

$$S_{\text{inf}} = -f \ln f - (1 - f) \ln (1 - f) \quad (3)$$

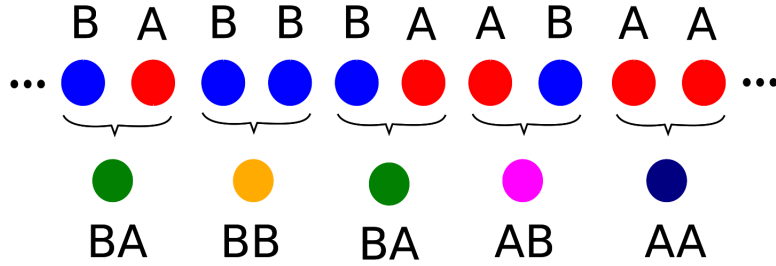


Figure 1: The same infinite sequence can be represented as composed of two types of beads A,B or as a one composed of four types of beads AA, AB, BA, BB.

The *information chemical potential* of species A is then

$$\mu_{\text{inf}} = -\frac{\partial S_{\text{inf}}}{\partial f} = \ln f - \ln(1-f) \quad (4)$$

If there is a finite sequence of length N in equilibrium with this infinite system then its grand potential depending on the number $N_A = \sigma N$ of A-segments in this sequence is

$$\frac{\Phi(\sigma)}{k_B T} = -N S_{\text{inf}}(\sigma) - \mu(f) N \sigma \quad (5)$$

And the probability to have $N_A = \sigma N$ segments is

$$\rho(\sigma) = \frac{1}{Z} e^{-\frac{\Phi(\sigma)}{k_B T}} = \frac{1}{Z} \left(\frac{f}{\sigma}\right)^{N\sigma} \left(\frac{1-f}{1-\sigma}\right)^{N-N\sigma} \quad (6)$$

Which is a binomial distribution.

Now let us consider an infinite sequence composed of dimers AA, AB, BB and BA (Figure 1). The entropy for this sequence is

$$S_{\text{inf}} = -p_{AA} \ln p_{AA} - p_{AB} \ln p_{AB} - p_{BA} \ln p_{BA} - p_{BB} \ln p_{BB} - S_0 \quad (7)$$

here S_0 appears as a reduction of entropy because p_{ij} are not independent. p_{ij} satisfy conditions $p_{AA} + p_{AB} + p_{BA} + p_{BB} = 1$, $p_{AB} = p_{BA} = \theta$, $p_{AA} + p_{BA} = f$ and $p_{BA} + p_{BB} = 1 - f$, where θ is the blockiness and f is the fraction of A units. The blockiness θ controls average lengths of blocks, because by definition it is a concentration of AB boundaries between blocks of

different types. In completely random copolymer $\theta = f(1-f)$ and the average length of the A-block is $\langle l \rangle = \frac{f}{\theta} = \frac{1}{1-f}$. If $\theta < f(1-f)$ then the sequence is depleted in AB and BA duplets and the copolymer is defined as *blocky*, the average lengths of A-blocks and B-blocks are larger than in random copolymer. Conversely, if $\theta > f(1-f)$ the concentration of AB and BA duplets is increased and the copolymer tends to be alternating, the average length of A and B-blocks is decreased. The maximum value the θ can take is $\min(f, 1-f)$. Of course we want to establish a relationship between θ and the parameter λ used in previous papers on correlated random copolymers.[15] According to definition, λ is the non-trivial eigenvalue of the transfer matrix (the trivial eigenvalue equals one), which in our notations takes the form:

$$\begin{pmatrix} \frac{p_{AA}}{f} & \frac{p_{BA}}{1-f} \\ \frac{p_{AB}}{f} & \frac{p_{BB}}{1-f} \end{pmatrix} = \begin{pmatrix} \frac{f-\theta}{f} & \frac{\theta}{1-f} \\ \frac{\theta}{f} & \frac{1-f-\theta}{1-f} \end{pmatrix} \quad (8)$$

Therefore, we get

$$\lambda = \frac{f - f^2 - \theta}{f(1-f)}, \quad (9)$$

which establishes a connection.

Returning to the information entropy and applying conditions on p_{ij} we get:

$$S_{\text{inf}} = -(f-\theta) \ln(f-\theta) - 2\theta \ln \theta - (1-f-\theta) \ln(1-f-\theta) - S_0 \quad (10)$$

In order to find S_0 we note that above expression should converge to Equation 3 when the sequence is random, i.e. $\theta = f(1-f)$. From this condition we find that $S_0 = -f \ln f - (1-f) \ln(1-f)$, so finally we have

$$\begin{aligned} S_{\text{inf}} = & -(f-\theta) \ln(f-\theta) - 2\theta \ln \theta - (1-f-\theta) \ln(1-f-\theta) + \\ & + f \ln f + (1-f) \ln(1-f). \end{aligned} \quad (11)$$

With this expression in hand we can calculate the chemical potentials:

$$\mu_f = -\ln f + \ln(1-f) + \ln(f-\theta) - \ln(1-f-\theta) \quad (12)$$

$$\mu_\theta = 2 \ln \theta - \ln(1-f-\theta) - \ln(f-\theta) \quad (13)$$

We can say that here A-monomers and AB-duplets are considered as quasiparticles and f and θ are their concentrations. For a distribution function for a chain with a finite length N ,

composition σ and blockiness t which is in equilibrium with infinite chain with composition f and blockiness θ , we get:

$$\begin{aligned}\rho(\sigma, t) &= \frac{1}{Z} e^{NS_{\text{int}}(\sigma, t) + \mu_f N\sigma + \mu_\theta Nt} = \\ &= \frac{1}{Z} \left(\frac{f}{\sigma}\right)^{-N\sigma} \left(\frac{1-f}{1-\sigma}\right)^{-N+N\sigma} \left(\frac{f-\theta}{\sigma-t}\right)^{N\sigma-Nt} \left(\frac{\theta}{t}\right)^{2Nt} \left(\frac{1-f-\theta}{1-\sigma-t}\right)^{N-N\sigma-Nt}\end{aligned}\quad (14)$$

Where Z is determined from the normalization condition

$$\int_0^1 d\sigma \int_0^{\min(\sigma, 1-\sigma)} \rho(\sigma, t) dt = 1 \quad (15)$$

If we reverse Stirling approximation again in analogy with binomial distribution, we can get:

$$\begin{aligned}\rho(\sigma, t) &= \frac{(N\sigma)!(N-N\sigma)!}{(N\sigma-Nt)!(Nt)!^2(N-N\sigma-Nt)!} \\ &\quad \frac{(f-\theta)^{N\sigma-Nt} \theta^{2Nt} (1-f-\theta)^{N-N\sigma-Nt}}{f^{N\sigma} (1-f)^{N-N\sigma}}\end{aligned}\quad (16)$$

In Appendix B we show another way to derive this distribution, which serves as additional support to the calculations presented above.

Example contour plots of the distributions are shown in Figure 2. We can see that at fixed value of N and f , the width of the distribution projected on the σ axes decreases as θ increases. We expected to see this, because difference in compositions between different chains expected to be larger when segments are arranged in blocks. If we compare two distributions with the same θ but different f we can see that the distribution with f closer to 0.5 is broader, so variations in composition are largest for symmetric copolymer.

III. MOMENT FREE ENERGY

Let us now consider a melt of random copolymers with distribution $\rho(\sigma, t)$ and write down a moment free energy for it.[24] We start with Flory-Huggins free energy for this melt:

$$\frac{F}{k_B TV} = \frac{1}{N} \int \rho(\sigma, t) \left(\ln \frac{\rho(\sigma, t)}{R_0(\sigma, t)} - 1 \right) d\sigma dt + \chi \rho_1 (1 - \rho_1) \quad (17)$$

where V is the volume of the system, χ is a Flory-Huggins parameter describing interactions of segments of type A and B and

$$\rho_1 = \int \sigma \rho(\sigma, t) d\sigma dt \quad (18)$$

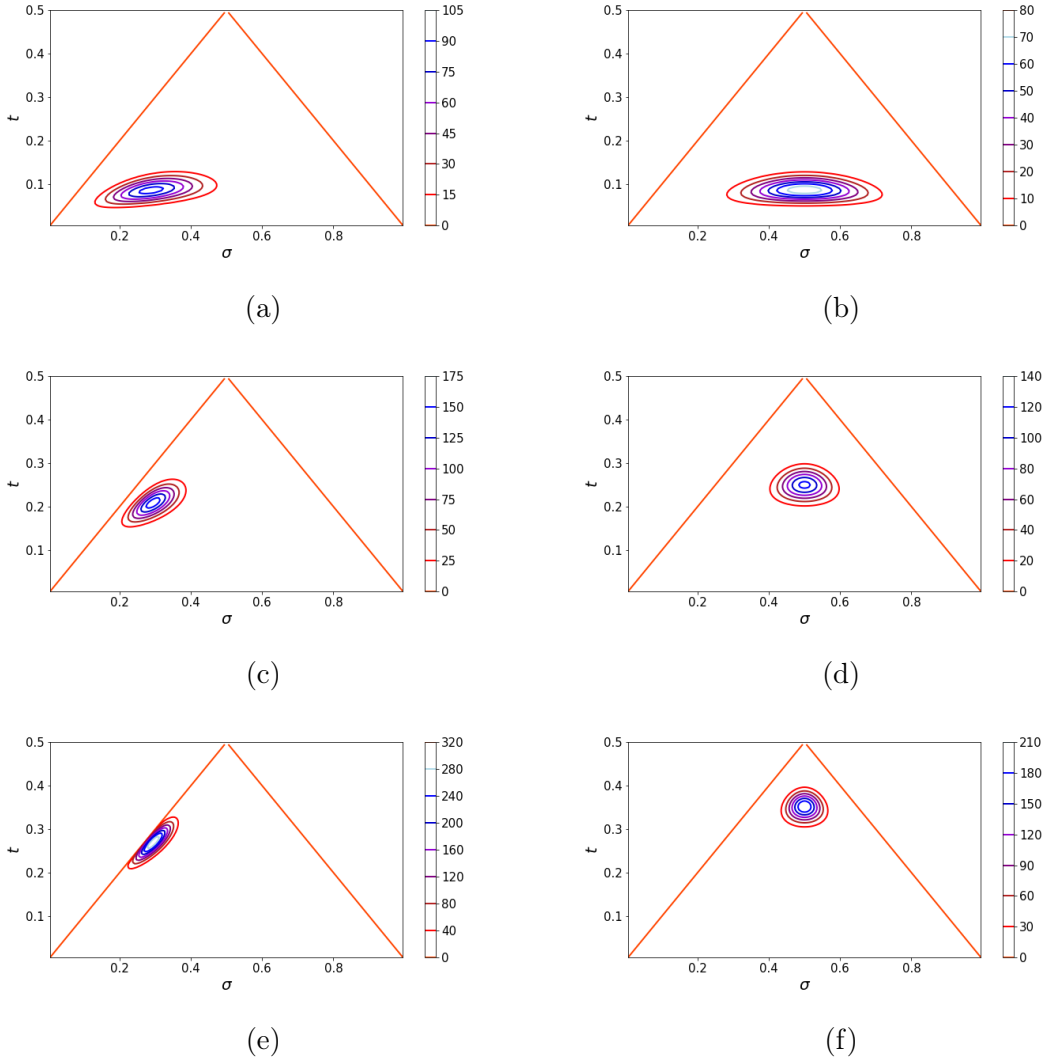


Figure 2: Distribution $\rho(\sigma, t)$ for copolymers characterised by $N = 100$ and (a) $f = 0.3$, $\theta = 0.09$ (blocky); (b) $f = 0.5$, $\theta = 0.09$ (blocky); (c) $f = 0.3$, $\theta = 0.21$ (random); (d) $f = 0.5$, $\theta = 0.25$ (random); (e) $f = 0.3$, $\theta = 0.27$ (alternating); (f) $f = 0.5$, $\theta = 0.35$ (alternating).

is the total volume fraction of A-monomers. $R_0(\sigma, t)$ is the distribution in the parent phase. It is added here for convenience as far as it represents a term linear in density $\rho(\sigma, t)$, which does not affect the phase behavior of a copolymer melt. We also implicitly assume that volumes of A and B segments are equal to each other, both segments are flexible, so that $\rho(\sigma, t)$ is simply a volume fraction of the polymer with parameters σ, t . [25]

Now we can apply the moments method [24] to reduce the number of degrees of freedom of the problem. We fix composition ρ_1 using Lagrange multiplier λ_1 along with the total volume

fraction which is equal to 1 with Lagrange multiplier λ_0 and the constrained free energy is minimized with respect to the remaining degrees of freedom:

$$\begin{aligned} \frac{F'}{kTV} = & \frac{1}{N} \int \rho(\sigma, t) \left(\ln \frac{\rho(\sigma, t)}{R_0(\sigma, t)} - 1 \right) d\sigma dt + \chi \rho_1 (1 - \rho_1) - \\ & - \lambda_0 \left(\int \rho(\sigma, t) d\sigma dt - 1 \right) - \lambda_1 \left(\int \sigma \rho(\sigma, t) d\sigma dt - \rho_1 \right). \end{aligned} \quad (19)$$

Minimizing with respect to $\rho(\sigma, t)$ we get

$$\rho(\sigma, t) = R_0(\sigma, t) e^{\lambda_0 + \lambda_1 \sigma}. \quad (20)$$

We can see that, in this approximation, all possible distribution functions in any coexisting phases belong to this family (equation 20). It is clear why we needed to include $R_0(\sigma, t)$ in the formula (equation 19), because the parent phase must be included in the family. The set of functions which are considered as candidates in coexisting phases can be extended by fixing high moments of the distribution. Next we substitute equation 20 into equation 19 and obtain expression for the moment free energy (omitting terms which are linear in ρ_0 and ρ_1):

$$F_m = \lambda_0 + \lambda_1 \rho_1 - \chi' \rho_1^2, \quad (21)$$

where $\chi' = \chi N$. Now we can analyse this expression as the free energy of a one-component system. However, in order to reproduce the phase diagram correctly above the cloud point more moments need to be fixed.

IV. PHASE DIAGRAMS

We expect that upon increase of the Flory-Huggins parameter χ' an initially uniform melt separates into two phases at a cloud point χ'_{cloud} , at which point a new phase with infinitesimal volume emerges. It is also expected the spinodal point of the system is located at some value of $\chi'_s > \chi'_{\text{cloud}}$. Beyond the spinodal point homogenous state can't exist as metastable.

To construct the phase diagram and to determine composition of coexisting phases from the moment free energies we write down standard equations for chemical potentials and osmotic pressures.

$$\mu_1 = \frac{\partial F_m}{\partial \rho_1} = \lambda_1 - 2\chi' \rho_1 \quad (22)$$

$$\pi = -F_m + \rho_1 \mu_{\rho_1} = -\lambda_0 - \chi' \rho_1^2. \quad (23)$$

Additionally, we have the condition that amounts of ρ_1 is conserved:

$$\rho_1^{(0)} = v_\alpha \rho_1^\alpha + (1 - v_\alpha) \rho_1^\beta \quad (24)$$

These equations can be solved by the standard Newton method with the set of unknowns $\{\lambda_1^\alpha, \lambda_1^\beta, v_\alpha\}$ instead of $\{\rho_1^\alpha, \rho_1^\beta, v_\alpha\}$ for convenience (see Appendix A for details). The spinodal point at which an initial homogeneous phase loses stability can be found from condition:

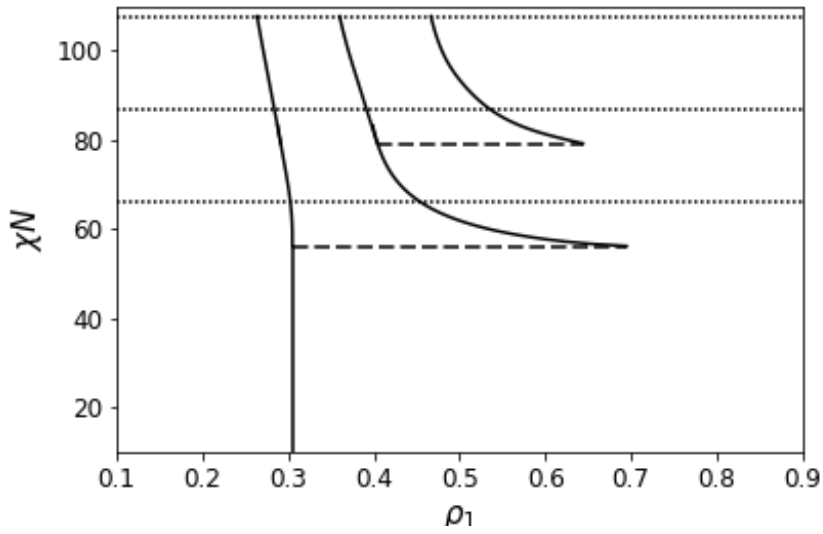
$$\frac{\partial^2 F_m}{\partial \rho_1^2} = \frac{\partial \lambda_1}{\partial \rho_1} - 2\chi'_s = \frac{1}{\rho_2 - \rho_1^2} - 2\chi'_s = 0, \quad (25)$$

which is a well known condition for the spinodal point in random copolymers. [11]

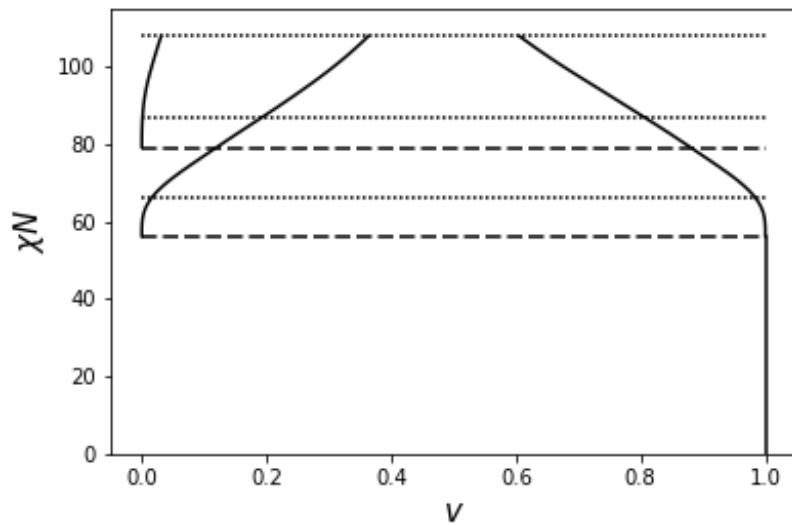
As far as it is not known in advance how many moments are needed to be fixed to produce a satisfactory approximation of the actual composition of the coexisting phases, we proceed by fixing an increasing number of moments at each step until phase diagram does not change any more for a given value of χN .

It can be added that in our calculations we have chosen to fix only the moments of composition, though for the 2D distribution which we use here there are also moments of blockiness and mixed moments. However, we found that fixing additional types of moments does not add any information to the phase diagrams, but significantly complicates calculations.

Figure 3a shows the phase diagram of a copolymer with fraction of A-units $f = 0.3$, blockiness $\theta = 0.09$ and chain length $N = 100$. Figure 3b is plotted to show the dependence of volume fractions of coexisting phases on χN . The binodal for separation of initially homogeneous phase into two phases is located at $\chi N = 56.17$. One of these phases is the cloud phase with composition equal to the initial composition of the system $\rho_1 = 0.305$. It occupies nearly all the system volume (see Figure 3b) and other is a shadow phase with composition $\rho_1 = 0.695$ and occupying an infinitesimal volume. Upon further increase in χN the composition of the shadow phase decreases strongly until it reaches the value $\rho_1 = 0.45$ at the spinodal point ($\chi N = 66.15$) corresponding to the instability point of initial homogeneous phase. The decrease of the composition of the second phase is a consequence of the increase of its volume fraction. If the volume fraction of a phase is sufficiently high its average composition inevitably is close to the composition of the initial phase because the initial distribution has one thin single peak. However, it is interesting to note the compositional contrast between



(a)



(b)

Figure 3: (a) Phase diagram for $f = 0.3$ and $\theta = 0.09$, $N = 100$ and 9 moments fixed. (b) volume fractions of coexisting phases. Spinodals are shown as dotted lines, cloud points are shown with broken lines.

phases above the spinodal. For example, at $\chi N = 70$ $\Delta\rho_1 \approx 0.13$ is larger than the variances of each phase $(\rho_2^\alpha - (\rho_1^\alpha)^2)^{1/2} = 0.0829$ and $(\rho_2^\beta - (\rho_1^\beta)^2)^{1/2} = 0.0831$ (noting that the vari-

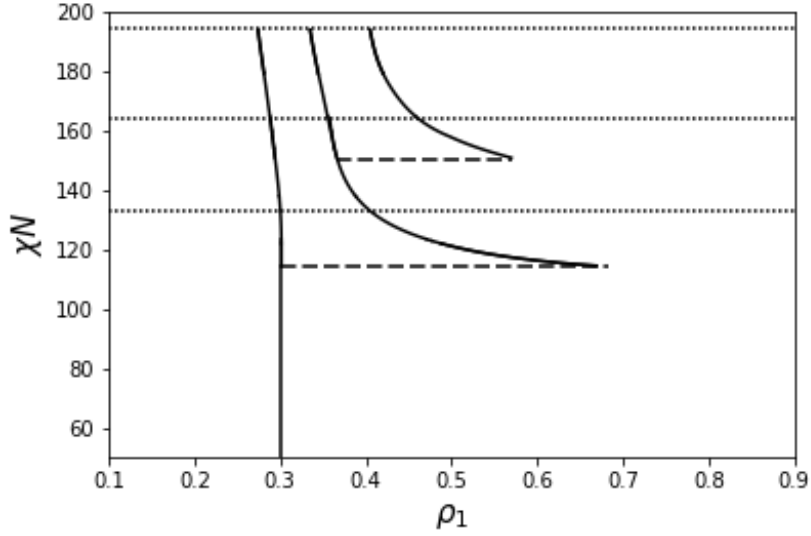


Figure 4: Phase diagrams for $f = 0.3$, $\theta = 0.15$ and $N = 100$ and 9 moments fixed. Spinodals are shown as dotted lines, cloud points are shown with broken lines.

ance of the parent phase is a bit larger and is equal in this case to $\left(\rho_2^\beta - (\rho_1^\beta)^2\right)^{1/2} = 0.0869$ meaning that they can be distinguished. At $\chi N = 79.18$ the second binodal with respect to coexistence of three phases is located and a new shadow phase emerges. The compositions of coexisting phases at this point are $\rho_1 = 0.29$, $\rho_1 = 0.4$ and $\rho_1 = 0.64$. At $\chi N = 86.68$ the first shadow phase loses its stability, which corresponds to the second spinodal point (phase compositions are $\rho_1 = 0.28$, $\rho_1 = 0.39$ and $\rho_1 = 0.54$). The next spinodal point is located at $\chi N = 107.7$ and here the shadow phase with largest ρ_1 loses stability and separates into two phases. However this fact is not reflected in Figure 3a.

The diagram in the Figure 3a is obtained from free energy with 9 moments of compositions fixed. It is enough to fix only the first moment to correctly predict the first cloud point. In order to predict correctly the location of the second spinodal point and volumes of coexisting phases at least 6 moments need to be fixed. And in order to predict location of the second cloud point at least 8 moments are required.

Figure 4 shows the phase diagram of a copolymer with composition $f = 0.3$, blockiness $\theta = 0.15$ and length $N = 100$, calculated with moment free energy depending on 9 moments of the distribution. The increased value of blockiness compared to the Figure 3a means that

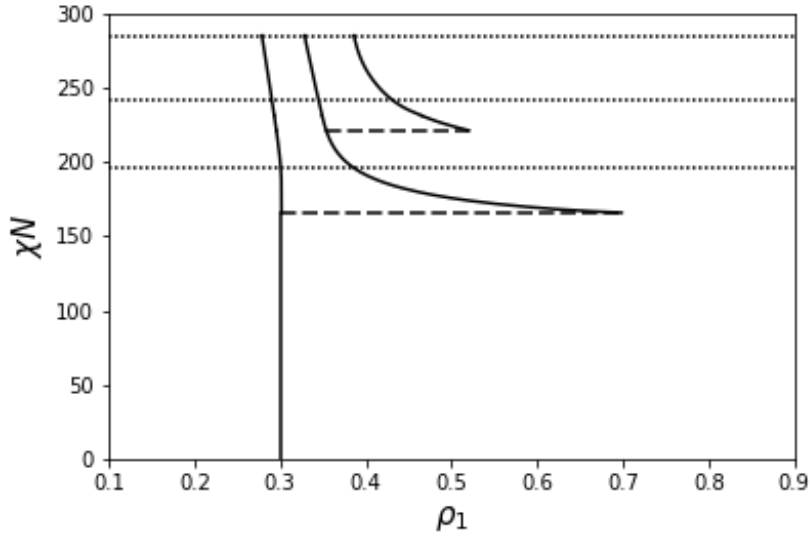


Figure 5: Phase diagrams for $f = 0.3$, $\theta = 0.09$ and $N = 300$ and 9 moments fixed.

Spinodals are shown as dotted lines, cloud points are shown with broken lines.

copolymer is less correlated. However, this value is still less than in a binomial copolymer with the same composition, i.e. $\theta = f(1 - f) = 0.21$. One can see that increase in blockiness leads both to an increase of the value of χN at which the first spinodal and the first cloud point are located. It is expected because an increase in blockiness leads to a decrease in the variance of the distribution, so increase of χN at spinodal point (equation (25)). The same reason explains why the distance between consecutive spinodals on the diagram increases and the compositional contrast decreases. Though the composition of a shadow phase at the first cloud point does not change ($f_{sh} = 1 - f$).

Figure 5 shows the effect of increasing N on phase diagram, it is calculated for a copolymer characterised by parameters $f = 0.3$, $\theta = 0.09$, $N = 300$. Interestingly, we can see that as we increase N both the first spinodal point χ_S and the first cloud point χ_C , with respect to separation into two phases slightly decrease and $\Delta\chi = \chi_S - \chi_C$ slightly increases.

Finally, Figure 6 shows a special case of a phase diagram for a system with critical composition $f = 0.5$. It differs from the phase diagrams for asymmetric copolymers. The first spinodal point coincides with the cloud point, and the transition from one phase to two phases is continuous. The composition of the two coexisting phases is symmetric with respect to the line $f = 0.5$ and their volume fraction does not change until the third phase emerges (Figure

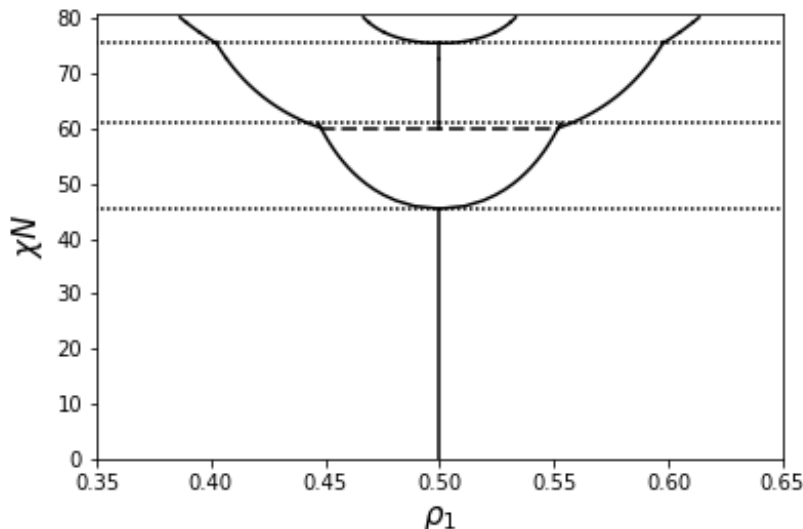


Figure 6: Phase diagrams for $f = 0.5$, $\theta = 0.09$ and $N = 100$ calculated with 9 moments fixed. Spinodals are shown as dotted lines, cloud points are shown with broken lines.

7). The transition from two phases to three phases is discontinuous. As χN increases the volume fraction of a phase with average composition $f = 0.5$ increases until the next spinodal line. The next transition is again continuous. These observations agree with observations of Nesarikar *et al.* [13] for binomial copolymers.

Figure 8 shows the dependence of cloud and spinodal points on composition and chain length. We can see, as expected, that both the spinodal and binodal increase with increasing asymmetry of composition. Slight decrease of both spinodal and binodal with N can be clearly also observed. The spinodal converges to the limit derived by Fredrickson *et al.*[15] for $N \rightarrow \infty$ (see Figures 9a and 9b)

$$\lim_{N \rightarrow \infty} \chi_S = \frac{\theta}{2f(1-f)(2f - 2f^2 - \theta)}. \quad (26)$$

In addition, there is a good correspondence with prediction for spinodal made in the same work for finite values of N . However, the Fredrickson's *et al.*[15] prediction for convergence of cloud points to spinodal points, $\chi_C \rightarrow \chi_S$, as $N \rightarrow \infty$ does not hold. Figure 10 shows that in fact the difference between the Flory-Huggins parameter at the cloud point and at spinodal point, $\Delta\chi = \chi_S - \chi_C$, is nearly independent on N . The reason for this discrepancy is an implicit assumption of the work[15] that distribution functions in all coexisting phases are

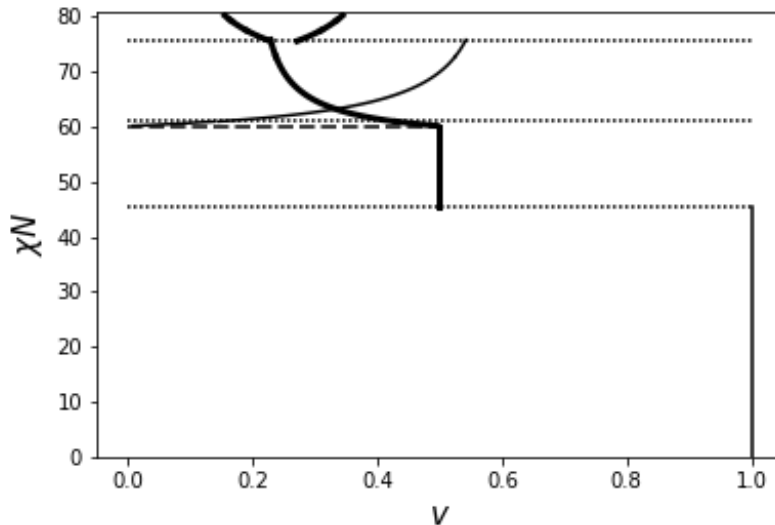


Figure 7: Phase diagrams for $f = 0.5$, $\theta = 0.09$ and $N = 100$ calculated with 9 moments fixed. Spinodals are shown as dotted lines, cloud points are shown with broken lines.

the same.

V. CONCLUSION

In this paper, we derive a probability distribution function for a *blocky* copolymer, with first-order Markov correlations along the sequence. Then we used this distribution with the method of moments by Sollich *et al.*[24] and Flory-Huggins theory to obtain phase diagrams of blocky copolymers.

This combination of methods allows one to calculate Flory-Huggins phase diagrams for copolymers characterised by arbitrary length and blockiness. Qualitatively obtained phase diagrams look similar to those for short binomial copolymers *et al.*[13]. Predicted compositional contrast between phases is larger than the width of the distributions of any coexisting phases, so in the framework of Flory-Huggins theory phases can be always distinguished. Our prediction for a spinodal are close to those made by Fredrickson *et. al.*[15] though they do not coincide with them except in the limit of infinite chain length $N \rightarrow \infty$. However, in contrast to previous predictions we showed that binodal does not converge to spinodal in the limit $N \rightarrow \infty$.

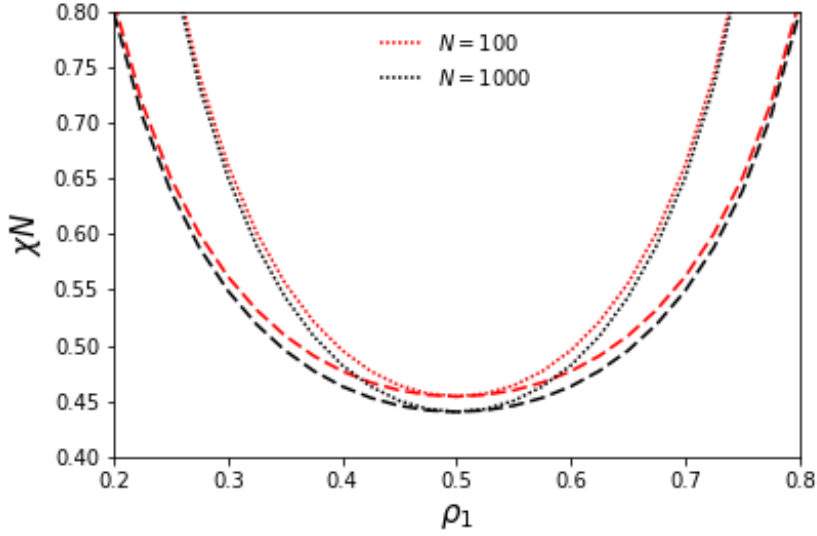


Figure 8: Dependence of spinodal points χ_S (dotted) and cloud points χ_C (dashed) at fixed values of $\theta = 0.09$ and (1) $N = 100$ (red), (2) $N = 1000$ (black)

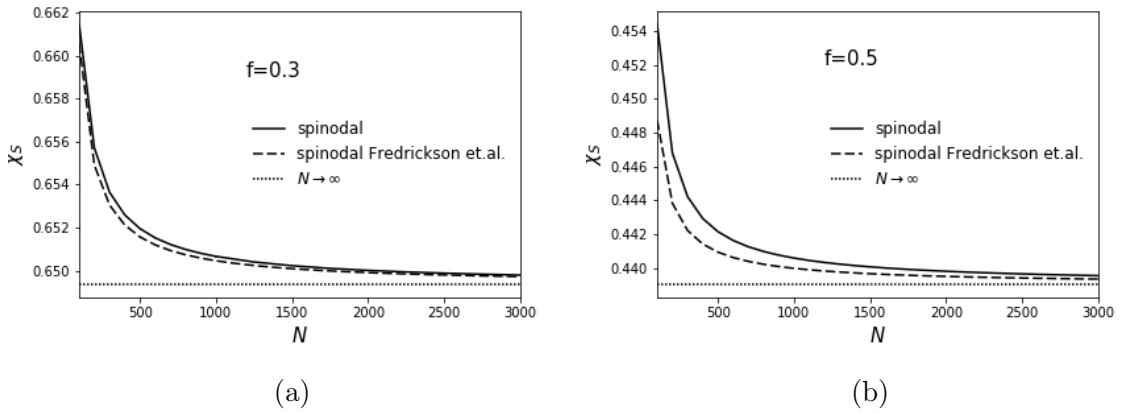


Figure 9: Spinodal points converge to the expression from the paper of Fredrickson *et al.*

$$\chi_S = \frac{1-\lambda}{2f(1-f)(1+\lambda)}. \text{(a) } f = 0.3, \theta = 0.09 \text{ (b) } f = 0.5, \theta = 0.09.$$

The strong feature of the present analysis is that fractionation is taken into account. It is expected that fractionation will affect all transitions occurring above the first cloud point, for example, formation of the microphase. Also, previously in the works using Landau expansion all one-chain correlation functions were calculated effectively for one infinite chain. Our approach allows to get more accurate result by averaging over the ensemble of different

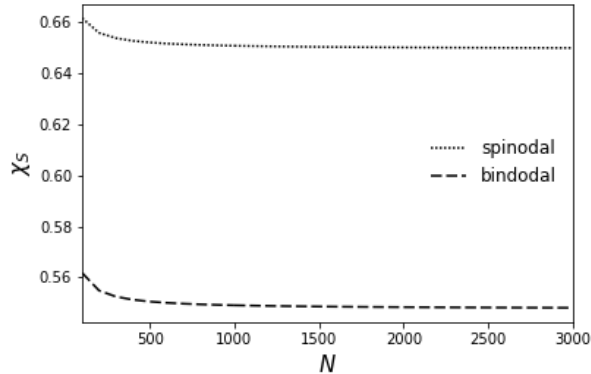


Figure 10: Dependence of spinodal points, χ_S , and binodal points, χ_C , on the length of the chain N for copolymer with $f = 0.3$, $\theta = 0.09$.

sequences. For example, for the scattering function we have:

$$S(k^2) = \sum_{\sigma,t} \rho(\sigma,t) S(k^2|\sigma,t) \quad (27)$$

Where $\rho(\sigma,t)$ is a distribution with respect to composition and blockiness and $S(k^2|\sigma,t)$ is a scattering function averaged over all sequences which have the same composition and blockiness. The calculation can be done not only for a parent phase, but also for all daughter phases as their distributions functions can be obtained with the method of moments.

From viewpoint of practical applications it is important to solve the problem about phase behavior of mixture of random copolymer with a plasticizer (solvent) in order to describe such system as a PVA film plasticized with polyols. This question was approached previously[24, 26], however only the case of non-selective solvent was considered. It seems promising to try to apply proposed methodology to tackle this problem.

APPENDIX A

In this section we include computation details. Considering the simplest case of moments free energy with one moment fixed and two phases in equilibrium. Then in order to determine compositions of these phases one needs to solve a system of equations:

$$f(x_n) = \{\mu_{\rho_1}^\alpha - \mu_{\rho_1}^\beta, \pi^\alpha - \pi^\beta, v_\alpha \rho_1^\alpha + (1 - v_\alpha) \rho_1^\beta - \rho_1^{(0)}\}^T = 0. \quad (28)$$

It is solved numerically with the Newton method: $x_{n+1} = x_n - f(x_n) [Df(x_n)]^{-1}$ where $x = \{\lambda_1^\alpha, \lambda_1^\beta, v_\alpha\}^T$ and:

$$\begin{aligned} (Df(x_n))_{ij} &= \frac{\partial (f(x_n))_i}{\partial (x_n)_j} = \\ &= \begin{pmatrix} \frac{\partial \mu_{\rho_1}^\alpha}{\partial \lambda_1^\alpha} & -\frac{\partial \mu_{\rho_1}^\beta}{\partial \lambda_1^\beta} & 0 \\ \frac{\partial \pi^\alpha}{\partial \lambda_1^\alpha} & -\frac{\partial \pi^\beta}{\partial \lambda_1^\beta} & 0 \\ v_\alpha \frac{\partial \rho_1^\alpha}{\partial \lambda_1^\alpha} & (1-v_\alpha) \frac{\partial \rho_1^\beta}{\lambda_1^\beta} & \rho_1^\alpha - \rho_1^\beta \end{pmatrix}. \end{aligned} \quad (29)$$

Derivatives with respect to Lagrange parameters are calculated as:

$$\frac{\partial \rho_1^{\alpha,\beta}}{\partial \lambda_1^{\alpha,\beta}} = \frac{\partial}{\partial \lambda_1^{\alpha,\beta}} \left(\frac{\int \sigma R_0(\sigma, t) e^{\lambda_1^{\alpha,\beta} \sigma + \beta_1 t} d\sigma dt}{\int R_0(\sigma, t) e^{\lambda_1^{\alpha,\beta} \sigma + \beta_1 t} d\sigma dt} \right) = \rho_2^{\alpha,\beta} - (\rho_1^{\alpha,\beta})^2 \quad (30)$$

$$\frac{\partial \lambda_0^{\alpha,\beta}}{\partial \lambda_1^{\alpha,\beta}} = \frac{\partial}{\partial \lambda_1^{\alpha,\beta}} \left(-\ln \left(\int R_0(\sigma, t) e^{\lambda_1^{\alpha,\beta} \sigma + \beta_1 t} d\sigma dt \right) \right) = -\rho_1^{\alpha,\beta} \quad (31)$$

All calculations were made using scripts written in Python with the *mpmath* package allowing arbitrary precision mathematics. All integrals were calculated with the trapezoidal rule and uniform discretization along the composition axis. For factorials Stirling approximation including a square root was used $n! \approx \sqrt{2\pi n} \cdot (n/e)^n$. The step along χN axes was varied to ensure convergence of the Newton solver and maximization of the computation speed.

As the function is peaked, discretization error and errors introduced by it into the values of moments are relatively high (notice also that the initial distribution is discrete as monomers cannot be divided, but we consider distribution as continuous, so may use discontinuities larger than N). However, the difference in energy between, for example, two and three phase coexistence is relatively low. So that if all free energies are calculated with one discretization (e.g. 50) and then compared with free energies calculated with the same discretization, then the result (for example, the preference of three phases over two phases at given χN) is the same for different discretizations (e.g. 50 and 100). However, when comparing free energies calculated with different discretizations between each other, then results can be arbitrary and phase diagrams might not be reproduced.

APPENDIX B

Consider again the binomial distribution:

$$\rho(N_A) = \frac{N!}{N_A!(N-N_A)!} f^{N_A} (1-f)^{N-N_A} \quad (32)$$

In this expression $f^{N_A} (1-f)^{N-N_A}$ gives the probability of a specific sequence ABABB... with total length N and the number of A-segments equals to N_A . And $\frac{N!}{N_A!(N-N_A)!}$ is the total number of sequences which has *the same description*, i.e. have a total length N and the number of A-segments equals to N_A . So, if we look at the distribution for a blocky copolymer

$$\rho(N_A, N_{AB}) = \frac{N_A!(N-N_A)!}{(N_A-N_{AB})!(N_{AB}!)^2(N-N_A-N_{AB})!} \cdot \frac{(f-\theta)^{N_A-N_{AB}} \theta^{2N_{AB}} (1-f-\theta)^{N-N_A-N_{AB}}}{f^{N_A} (1-f)^{N-N_A}}, \quad (33)$$

we can see that it has the same structure as the binomial distribution and the probability of a specific sequence, ABABB..., in which we calculated both the number of A-segments, N_A , and the number of AB-duplets, N_{AB} equals to

$$p(ABABB...) = \frac{(f-\theta)^{N_A-N_{AB}} \theta^{2N_{AB}} (1-f-\theta)^{N-N_A-N_{AB}}}{f^{N_A} (1-f)^{N-N_A}}. \quad (34)$$

So, if we calculate the probability of $ABBB$ sequence (it is short here for simplicity), we have:

$$p(ABBB) = p_A \cdot P_{AB} P_{BB} P_{BB} = f \cdot \frac{\theta}{f} \frac{1-f-\theta}{1-f} \cdot \frac{1-f-\theta}{1-f} = \frac{\theta(1-f-\theta)^2}{(1-f)^2} \quad (35)$$

where P_{IJ} are corresponding elements of transfer matrix (8) From the formula above (34) we obtain:

$$p^*(ABBB) = \frac{\theta^2(1-f-\theta)^2}{f(1-f)^3} \quad (36)$$

So we have a discrepancy between $p(ABBB)$ and $p^*(ABBB)$. The contradiction is resolved if we take into account that in equation 34 no start of the sequence was ever specified and it must be "cyclic" without cyclic symmetry. So in order to obtain the probability for a linear sequence we need to specify a starting segment and remove one duplet adjacent to it (in this particular case the BA-duplet):

$$p(ABBB) = p^*(ABBB) \cdot \frac{P_A}{P_{BA}} \quad (37)$$

However, this end-chain effects will be unimportant in the limit of large N , N_A and N_{AB} .

The second part of the distribution, the number of sequences with the same description N , N_A and N_{AB} , can be calculated in the following way. Assuming that we have a string of A-s with length N_A and a string of B-s with length $N - N_A$. Then if we want to mix them in a way such that there are precisely $N_{BA} + N_{AB} = 2N_{AB}$ boundaries between A and B-blocks, we need to find a number of ways in which one can split a continuous A-string into N_{AB} blocks and for each of this splits find a number of ways the B-string can be split into N_{AB} blocks. Which means that the total number of combinations is:

$$\frac{N_A!}{(N_A - N_{AB})!N_{AB}!} \cdot \frac{(N - N_A)!}{(N - N_A - N_{AB})!N_{AB}!} \quad (38)$$

This expressions coincides with the number of sequences with the same description from the distribution in equation 33. In this case end-chain effects are also neglected as the number of boundaries $2N_{AB}$ is even, implying that all beads are located on a "circle".

It is interesting to note that distribution in equation 33 converges exactly to binomial distribution in case when $\theta = f(1 - f)$ and the summation over N_{AB} is taken. This happens because for binomial distribution there is no difference between a linear chain model with ends and the circle model considered above without ends, as there are no correlation between probability of appearance of different segments.

ACKNOWLEDGMENT

The authors would like to thank Procter and Gamble and the UK research council, EPSRC for funding through grant EP/P007864/1 "Molecular Migration in Complex Matrices: Towards Predictiv Design of Structures Products".

-
- [1] R. K. Tubbs, E. I, and P. D. Nernours, *J. Polym. Sci. Part A-1* **4**, 623 (1966).
 - [2] Y. I. Denisova, L. B. Krentsel', A. S. Peregudov, E. A. Litmanovich, V. V. Podbel'skiy, A. D. Litmanovich, and Y. V. Kudryavtsev, *Polymer Science - Series B* **54**, 375 (2012).
 - [3] Y. I. Denisova, G. A. Shandryuk, L. B. Krentsel', I. V. Blagodatskikh, A. S. Peregudov, A. D. Litmanovich, and Y. V. Kudryavtsev, *Polymer Science - Series A* **55**, 385 (2013).

- [4] O. Squillace, R. Fong, O. Shepherd, J. Hind, J. Tellam, N. J. Steinke, and R. L. Thompson, *Polymers* **12**, 1 (2020).
- [5] A. Briddick, R. J. Fong, E. F. Sabattié, P. Li, M. W. Skoda, F. Courchay, and R. L. Thompson, *Langmuir* **34**, 1410 (2018).
- [6] R. Ergun, J. Guo, and B. Huebner-Keese, *Encyclopedia of Food and Health*, 694 (2015).
- [7] M. B. Karimi, F. Mohammadi, and K. Hooshyari, *International Journal of Hydrogen Energy* **44**, 28919 (2019).
- [8] P. I. Teixeira, D. J. Read, and T. C. McLeish, *Journal of Chemical Physics* **126** (2007), 10.1063/1.2437200.
- [9] O. V. Noah, A. D. Litmanovich, and N. A. Platé, *Journal of Polymer Science: Polymer Physics Edition* **12**, 1711 (1974).
- [10] J. M. Kim, S. B. Chakrapani, and B. S. Beckingham, *Macromolecules* (2020), 10.1021/acs.macromol.0c00526.
- [11] R. L. Scott, *J. Polym. Sci.* **9**, 423 (1952).
- [12] B. J. Bauer, *Polym. Eng. Sci.* **25**, 1081 (1985).
- [13] A. Nesarikar, M. Olvera De La Cruz, and B. Crist, *The Journal of Chemical Physics* **98**, 7385 (1993).
- [14] E. Shakhnovich and A. Gutin, *Journal de Physique* **50**, 1843 (1989).
- [15] G. H. Fredrickson, S. T. Milner, and L. Leibler, *Macromolecules* **25**, 6341 (1992).
- [16] A. V. Dobrynin and I. Y. Erukhimovich, *JETP Lett.* **53**, 570 (1991).
- [17] H. Angerman, G. Brinke, and I. Erukhimovich, *Macromolecules* **29**, 3255 (1996).
- [18] G. Vanderwoude and A. C. Shi, *Macromolecular Theory and Simulations* **26**, 1 (2017).
- [19] E. N. Govorun and A. V. Chertovich, *Journal of Chemical Physics* **146** (2017), 10.1063/1.4973933.
- [20] S. V. Panyukov and I. I. Potemkin, *JETP Lett.* **64**, 197 (1996).
- [21] A. Subbotin and A. Semenov, *The European Physical Journal E* **7**, 49 (2002).
- [22] A. Von Der Heydt, M. Müller, and A. Zippelius, *Physical Review E - Statistical, Nonlinear, and Soft Matter Physics* **83**, 1 (2011).
- [23] A. V. D. Heydt, M. Marcus, and A. Zippelius, *Macromolecules* **43**, 3161 (2010).

- [24] P. Sollich, P. B. Warren, and M. E. Cates, in *Advances in Chemical Physics* (John Wiley & Sons, Ltd, 2007) pp. 265–336.
- [25] Note1, Phase behavior of stiff copolymers in the framework of wormchain model was recently studied by the group of A. J. Spakowitz, for example [?].
- [26] S. Mao, Q. Macpherson, C. Liu, and A. J. Spakowitz, *Macromolecules* **51**, 4167 (2018).